Geomechanics and Engineering, *Vol. 17, No. 2 (2019) 119-131*
DOI: https://doi.org/10.12989/gae.2019.17.2.119

Examination of 3D long-term viscoplastic behaviour of a CFR dam using special material models

Memduh Karalar[a] and Murat Çavuşli*

Department of Civil Engineering, Zonguldak Bulent Ecevit University, Zonguldak, Turkey

(Received March 31, 2018, Revised December 1, 2018, Accepted December 24, 2018)

Abstract. Time dependent creep settlements are one of the most important causes of material deteriorations for the huge water structures such as concrete faced rockfill dams (CFRDs). For this reason, performing creep analyses of CFRDs is vital important for monitoring and evaluating of the future and safety of such dams. In this study, it is observed how changes viscoplastic behaviour of a CFR dam depending the time. Ilısu dam that is the longest concrete faced rockfill dam (1775 m) in the world is selected for the three dimensional (3D) analyses. 3D finite difference model of Ilısu dam is modelled using FLAC3D software based on the finite difference method. Two different special creep material models are considered in the numerical analyses. Wipp-creep viscoplastic material model and burger-creep viscoplastic material model were rarely used for the creep analyses of CFRDs in the last are taken into account for the concrete slab and rockfill materials-foundation, respectively. Moreover, interface elements are defined between the concrete slab-rockfill materials and rockfill materials-foundation to provide interaction condition for 3D model. Firstly, dam and foundation are collapsed under its self-weight and static behaviour of the dam is evaluated for the empty reservoir conditions. Then, reservoir water is modelled considering maximum water level of the dam and time-dependent creep analyses are performed for maximum reservoir condition. In this paper, maximum principal stresses, vertical-horizontal displacements and pore pressures that may occur on the dam body surface during 30 years (from 2017 to 2047) are evaluated in detail. According to numerical analyses, empty and maximum reservoir conditions of Ilısu dam are compared with each other in detail. 4 various nodal points are selected under the concrete slab to better seen viscoplastic behaviour changes of the dam and viscoplastic behaviour differences of these points during 30 years are graphically presented. It is clearly seen that horizontal-vertical displacements and principal stresses for maximum reservoir condition are more than the empty reservoir condition of the dam and significant pore pressures are observed during 30 years for maximum reservoir condition. In addition, horizontal-vertical displacements, principal stresses and pore pressures for 4 nodal points obviously increased until a certain time and changes decreased after this time.

Keywords: burger-creep viscoplastic model; concrete faced rockfill dam; deformation-stress behavior; interface element; wipp-creep viscoplastic model

1. Introduction

Water has always been the life source for all living creatures since the world has been existed. Mankind has built many water constructions until present days to continue their lives. One of these important water structures is the dam. Today, many dam types are constructed (e.g., rockfill dams, concrete dams) and one of them is concrete faced rockfill (CFR) dam. CFR dams are widely preferred in Turkey and worldwide due to their short construction time, cheap cost, their excellent resistance to leakage, stress and settlement. While constructing CFR dams, the rockfill materials are compacted in layers and a concrete slab is constructed on the front face of the dam body to prevent leakage. This concrete slab works like an impermeable layer and the rock fill body supports to the concrete surface plate by providing balance of dam. These dams must be constantly monitored and carefully analyzed in order to obtain important information on the safety and the future.

Settlement is one of the most important deformation characteristics for high CFR dams and it is regarded as a key indicator for safety of these dams. Generally, there are two different types of deformations associated with these dams. First one is the vertical displacement that occur under the dam's own weight and second one is the horizontal deformations which are perpendicular to the main axis of the dam. From past to present day, many researchers have investigated these dams. Soydemir and Kjaernsli (1979) proposed a technique for predicting the settlements of CFR dams after 10 years of operation. Then, Clements (1984) edited this prediction technique that was proposed by Soydemir and Kjaernsli. Kovacevic *et al.* (1994) and Duncan (1996) contributed to developments for embankment and rockfill dam's deformation behaviors. Naylor (1997) suggested many important methods to incorporate settlements of rockfill into constitutive models. Besides, Fenves (1998) investigated plastic-damage model for cyclic loading of concrete structures. A new plastic-damage model for concrete slab of CFR dams is developed using the concepts of fracture-energy-based damage and

*Corresponding author, Graduate Research Assistant
E-mail: murat.cavusli@beun.edu.tr
[a]Assistant Professor

http://www.techno-press.org/?journal=gae&subpage=7 ISSN: 2005-307X (Print), 2092-6219 (Online)

stiffness degradation. Zhang *et al.* (2004) investigated a high concrete faced rockfill dam. It was proposed a contact analysis method and time dependent analyses were performed. It was revealed in that study whether the deformation of the CFR dam body is nonlinear or time dependent. Yu *et al.* (2005) examined 3D effects of some major factors on the stability of an earth-rockfill dam. These factors are topography of the canyon and geometrical characteristics of the dam. It was suggested that it has to be careful to the canyon shape, gradient of the dam slope and height of the dam while performing 3D numerical analyses of the CFR dams. Albaa *et al.* (2008) focused on displacement of the dam body and reservoir slopes. Dam deformations were evaluated using terrestrial interferometric techniques. Seo *et al.* (2009) examined behavior of CFR dams during initial impoundment. The numerical results showed that face slab deformation is more influenced by transition zone stiffness than face slab stiffness, supporting the centrifuge results. Bayraktar *et al.* (2009) investigated the effect of hydrostatic pressure on nonlinear behaviour of CFR dam. It was revealed in that study the hydrodynamic pressure of the reservoir water leads to increases in the maximum displacements and principal stresses of the dam. Fang and Liu (2011) performed stress-strain analyses of a rockfill dam. It was indicated that especially after the foundation treatment, the displacement of the dam foundation clearly diminishes and it is well beneficial for the functioning of the core. Zhou *et al.* (2011) examined the settlement analysis of CFR dam. A creep model was used to model the rockfill during period of dam operation. Time dependent settlement behaviour of the CFR dam was studied with situ settlement-monitoring records and displacement back analysis. It was shown in that study settlements on the dam body surface increase in the dam body depending to the time. Dakoulas (2012) investigated nonlinear seismic response of CFR dams that were constructed on the narrow canyons. It was indicated that dynamic rockfill settlements increase compression and decrease tension in the concrete slab. Xu *et al.* (2012) performed 3D simulation based on a modified generalized plasticity model and CFR dam was monitored in detail. Numerical analyses and monitoring records were compared in that study and numerical results agreed well with in situ monitoring records of the dam settlement. Zou *et al.* (2013) examined a CFR dam considering a generalized plasticity model. The numerical results of that study shows that a 3D finite element procedure based on a generalized plasticity model can be used to assess the responses of CFRDs. Kim *et al.* (2014) used a nonlinear and inelastic constitutive soil model to represent the behaviour of CFR dam material. Finite elements analyses were performed to assess the displacements during both the construction and initial reservoir filling stages. The vertical and horizontal displacements increased along the height of the dam body for filling stages when compared with construction stage. Xu *et al.* (2015) evaluated dynamic damage on the slabs of CFR dam using the plastic-damage model. During a strong earthquake, numerical simulations of the construction stage, impoundment process, and seismic excitation were performed to examined the tensile damage development in the concrete slab of a CFR dam. Mahinroosta *et al.* (2015) investigated the simulation of the settlement of first filling an a rockfill dam and nonlinear behaviour of the dam was observed in detail. Significant principal stresses and horizontal-vertical displacements were acquired in the dam body for first reservoir water filling and the behaviour of the dam clearly changed depending to the time. Zhou *et al.* (2016) examined numerical analyses of soft longitudinal joints in CFR dam. It was revealed that soft joints can significantly reduce the axial stress of face slab. Moreover, displacements and principal stresses in the dam body were observed in that study. Guo *et al.* (2016) proposed a method of deformation back analysis based on the response surface method and genetic optimization theory for the creep analysis of the high rockfill dams. Time dependent settlements in the dam body were obtained and the performance of the rockfill dam was estimated. Xu *et al.* (2017) performed the concrete slab dynamic damage analysis of CFRDs considering concrete nonuniformity. Dam was analyzed using two-dimensional finite-element method. Numerical results showed that when the randomness of material parameters of the concrete slab was not taken into account, the stress of the face slab along the slope direction was larger at ～0.65-0.85H (H is the dam height). Rashidi and Haeri (2017) evaluated the behavior of the rockfill dams during construction and initial impounding using the numerical modeling and the instrumentation data. For this purpose, finite difference model was modelled using FLAC software. Strain-hardening and strain-softening models were modified based on the data obtained from laboratory experiments and time dependent deformation-stress behaviour of the dam was acquired in detail. Baak *et al.* (2017) examined stability analysis on the concrete slab of the highest CFR dam in South Korea. In that study, a 125 m high CFR dam in South Korea was simulated with a software. The interaction properties of the concrete slab were estimated based on a comparison to monitored vertical displacement history obtained from the concrete slab. Prampthawee *et al.* (2017) performed the time-dependent analyses for high rockfill dam. 3D finite element analyses without creep and with creep considerations of rockfill dam were performed and compared with the situ measurements. Settlement and principal stress-strain of the dam body were obtained depending the time. Wen *et al.* (2017) performed 3D numerical analyses and behaviour of the dam was monitored with a detailed deformation-monitoring system. Time dependent 3D settlements in the dam body were observed according to numerical analyses and settlements and principal stresses of the dam were evaluated. Pang *et al.* (2018) evaluated stochastic seismic performance assessment of CFRDs based on generalized probability density evolution method. That study demonstrated that this density method has a good applicability to seismic performance assessment of high CFRDs. Pang *et al.* (2018) performed seismic reliability evaluation of earth-rockfill dams considering generalized probability density evolution method. A new and important method was presented to assess the seismic reliability of earth dams. Numerical results showed that this method is an effective approach to evaluate seismic reliability of these dams. Moreover, Pang *et al.* (2018) extended a seismic fragility analysis method based on incremental dynamic analysis (IDA) to assess the seismic performance of CFRDs. That study demonstrated that this method can provide strong scientific basis for predicting the earthquake behaviour of high CFRDs. When examined these studies, Wipp and Burger creep material models have not been used in the past to evaluate the viscoplastic creep behaviour of the CFR dams. Moreover, long-term vertical displacement, horizontal displacement, principal stress and pore pressure behavior of CFR dams have not been graphically compared with each other in the literature. Finally, there are no studies about the time depending future estimation of CFR dams. Thus, this study is very important and very critical to assess the effect of these special viscoplastic material models on the time dependent creep behaviour of the CFR dams and to compare long-term viscoplastic behaviour of these dams.

2. Scope of the study

Monitoring of CFR dam's creep behaviour during all stages of its life is vital importance for safety and future of these dams. For this purpose, Ilısu dam that was constructed on the Tigris River in South-eastern of Turkey is selected for three dimensional (3D) time dependent analyses and it is modelled using FLAC3D software based on the finite difference method. Special material models for time dependent creep analysis are taken into account for different materials of the dam in the viscoplastic numerical analyses. Burger-creep viscoplastic model that is used to simulate the visco-elastoplatic creep process of geological materials and corresponds to the Mohr-Coulomb material model is used for rockfill materials and foundation in this study. The Drucker Prager model is widely used for frictional materials such as rock and concrete and this material model is the most compatible with the WIPP-reference creep law. Because both models are formulated in terms of the second invariant of the deviatoric stress tensor (Itasca, 2002). Thus, Wipp- creep viscoplastic model is defined for concrete slab in numerical analyses using special fish functions. These material models were rarely used for analyzing of creep behaviour of CFR dams in the literature. One of the most important purposes of this study is to examine the effect of these special material models on the time dependent creep behaviour of Ilısu CFR dam. This examination will provide many contributions to the literature. Moreover, interface elements are taken into account between the concrete slab-rockfill material and the rockfill material-foundation to obtain interaction condition between discrete surfaces. Another important aim of this study is to investigate the effect of these interface elements on the viscoplastic behaviour of the CFR dams. Future behaviour estimation of CFR dams is one of the most important aims for this paper. The reservoir water is modelled by considering the maximum reservoir water height (120 m). Numerical analyses are performed for empty and maximum reservoir condition of the Ilısu dam to observe the long-term principal stress, displacement, pore-pressure changes in the dam body. These numerical results are compared according to numerical analyses and important information has been obtained about how the Ilısu CFR dam will behave in the future.

3. Ilısu concrete faced rockfill dam

The Ilısu Dam is the part of the Southeastern Anatolian Project (GAP) and it is currently the largest hydropower project in Turkey. This construction was completed in 2017 year and the project area is between Siirt, Batman and Diyarbakir provinces. Dam was built in the boundaries of the Ilısu village. This dam which is the longest concrete faced rockfill dam in the world has 1775 m crest length. In addition, this structure is one of the largest rockfill dam in the world now. The project includes totally 24 million m^3 filling material, 3 diversion tunnels with a diameter of 12 m and length of 1 km, 3 power tunnels with a diameter of 11 m. Dam's precipitation area is 35509 km^2. The crest width is 8 m and dam body height is 130 m. The lake volume is 10.4 billion m^3. Maximum water elevation is 526.82 m and reservoir area is 318.5 km^2. The project will generate 3.833 GWh power per year in average with an installed capacity of 1.200 MW. Ilısu dam's location is showed in detail in Fig. 1. In addition, the depth of the dam body changes along the crest of the dam. The slope of the upstream and downstream are 1:1.4 and slopes of the rockfill zones and transition zones are 2:1.5. The typical cross section of Ilısu dam and details of the dam body height are demonstrated in Fig. 2.

The project of Ilısu CFR dam was started in 1950. However, the main project of the dam was created in 1982. Firstly, Ilısu dam was planned as a clay core rockfill dam that have 45000000 m^3 filling materials. This plan was changed in 2007 as a concrete face rockfill dam. Thus, dam body volume was reduced to 24000000 m^3 and construction time of the dam was very shortened. The dam body excavation of the Ilısu dam was started in 2011.

7500000 m^3 rock materials were excavated from under the dam body to reach the main rock and dam body was

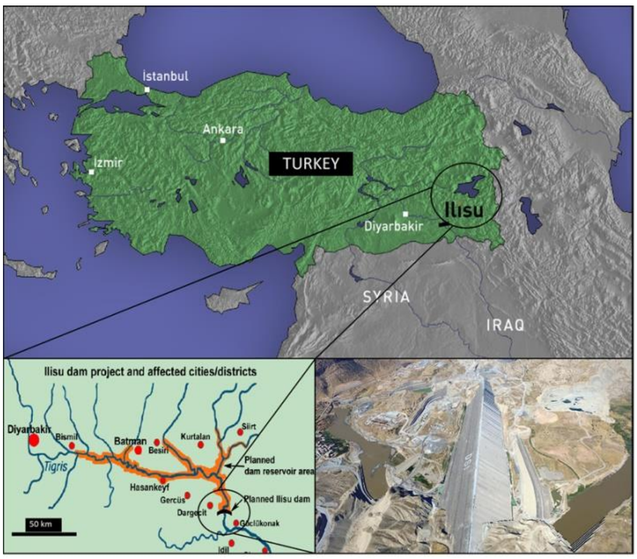

Fig. 1 The location and view of Ilısu Dam

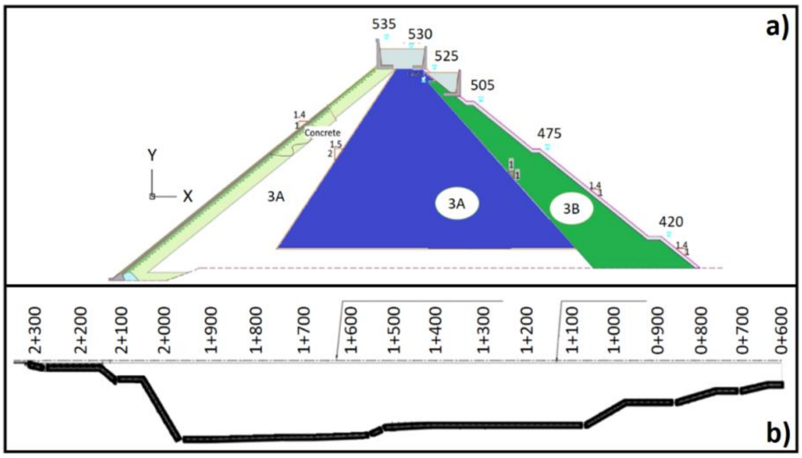

Fig. 2 (a) The typical cross section of Ilısu dam and (b) change of dam body height along crest axis (DSI 2018)

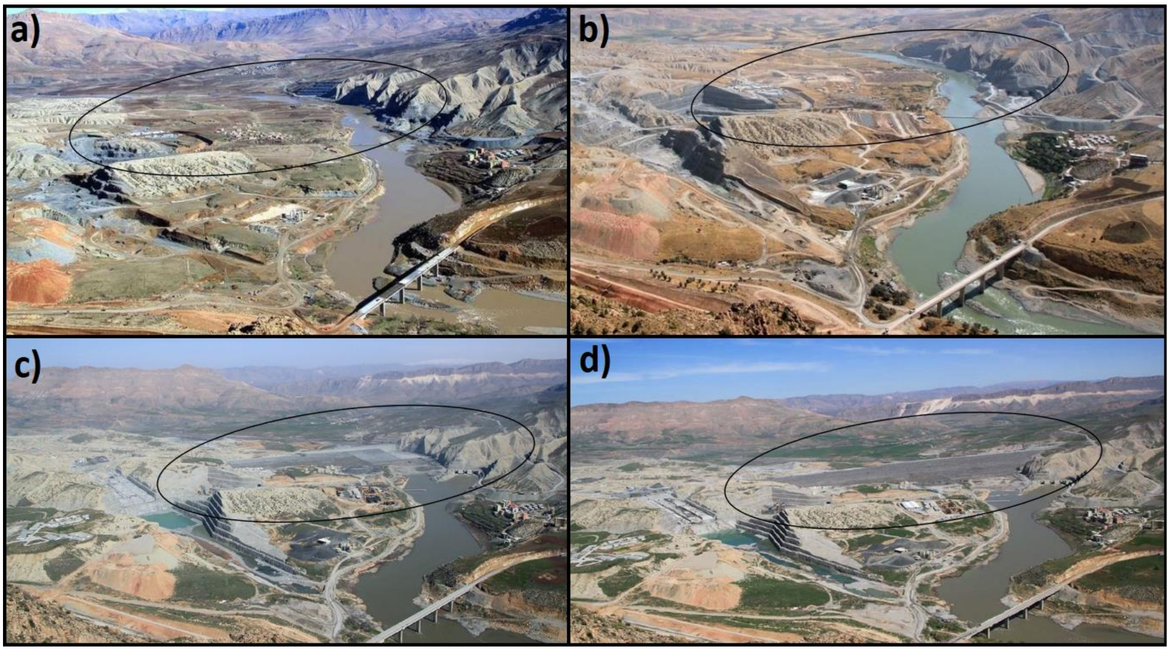

Fig. 3 Project area of Ilısu CFR dam (a) in 2011, (b) in 2012, (c) in 2013 and (d) in 2014

Table 1 Material properties of Ilısu Dam body (DSI 2018)

Characteristics	Specify weight	Unit Weight	Porosity	Water content	Air content	Material content
Unit	g/cm^3			%		
2B	2.74	2.23	18.61	4.05	14.56	81.39
3A	2.68	1.99	25.75	7.78	17.97	74.25
3B	3.01	2.25	25.25	1.50	23.75	74.75

completely placed on the strong rock. Construction steps of Ilısu dam are shown in Fig. 3 in detail. Moreover, Ilısu dam, which started to hold water in 2014, reached its maximum water level in 2017.

The Ilısu dam was built as concrete faced rockfill dam and it was constructed using many different rockfill materials. While constructing Ilısu dam, rockfill materials were compacted by sheepsfoot rollers. This dam has 3 different filling materials such as basalt (3B), limestone (3A), bedding zone (2B) and a concrete slab was constructed on the surface of the dam. All filling materials have different mechanical properties and mechanical properties of the materials are selected from the laboratory experiments for numerical analyses as given in Table 1.

4. Three dimensional modelling of Ilısu CFR dam

Ilısu dam which is one of the most important rockfill dams in Turkey is selected for 3D creep analyses and it is modelled using FLAC3D software to examined the viscoplastic behaviour of the dam in detail. The details of the 3D finite difference model are shown in Fig. 4.

In Fig. 4, constructing process of 3D model of the dam is shown in detail. While modeling this structure, the concrete slab which is constructed to prevent leakage on the dam surface, rockfill materials and foundation are modelled as the project of the Ilısu dam. The finite difference model of the dam has 5 different sections. Different sections which have various geometries generate the 4 different blocks and these blocks are merged to obtained the 3D finite difference

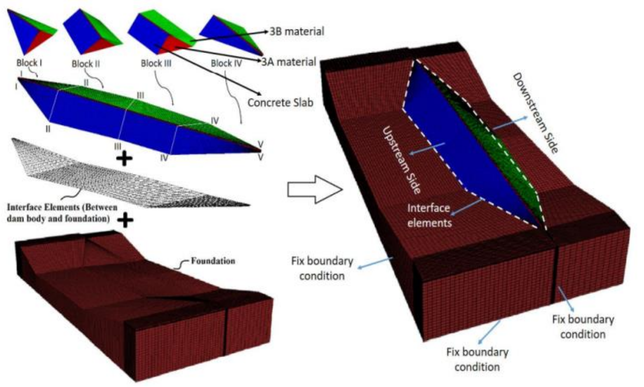

Fig. 4 View of blocks and 3D finite difference model of Ilısu Dam

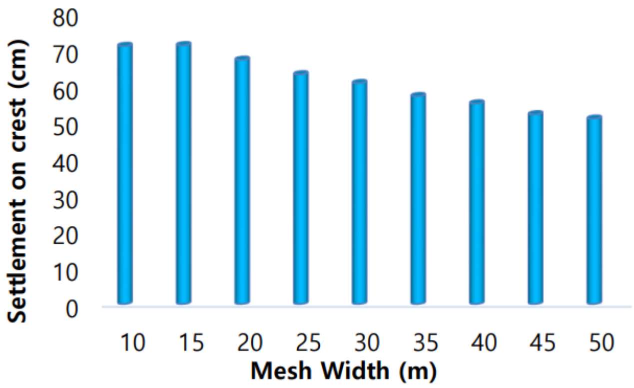

Fig. 5 Settlement changes of the crest for different mesh widths

model of the dam body. Details of sections and blocks are shown in Fig. 4. After dam body is modelled, the foundation is extended toward downstream and the valley side as much as dam height. Also, it is extended three times of the dam height at upstream side of dam. Finally, height of the foundation is considered as much as the dam height. These lengths are not randomly considered for 3D model. The most critical conditions for the length and the height of the reservoir water, dam body, downstream and side sections are as indicated above (Kartal *et al.* 2017). Total 1304547 finite difference elements are used in 3D finite difference model. Special material models are taken into account for the materials of the dam in the numerical analyses. Burger-creep viscoplastic model which is considered to simulate the viscoplastic creep behaviour of geological materials is taken into account for the rockfill materials and foundation (Zou *et al.* 2013). The Drucker Prager model is widely used for frictional materials such as rock and concrete. This material model is the most compatible with the WIPP-reference creep law because of both models are formulated in terms of the second invariant of the deviatoric stress tensor (Itasca 2002). Thus, Wipp-creep viscoplastic model is considered for the concrete slab using fish code which is specially defined to FLAC3D software. Moreover, interface elements are used between discrete surfaces to provide interaction condition. Finally, the reservoir water is modelled for the maximum reservoir water height (120 m). The effect of the leakage on the viscoplastic behaviour of the dam is taken into account using water table and hydrostatic water loads (Li and Desai, 1983). Movements of the boundaries of the 3D model must be restricted before 3D model is analyzed. So, the movement of the bottom of the foundation is restricted in three directions (x, y, z). Moreover, the movement of the side surfaces of the model is allowed only in the vertical direction (z) and it is restricted in the horizontal directions (x, y). The Ilısu dam has a great number of elements and nodes. So, the creating and meshing of the 3D model took a long time. Many problems are encountered during viscoplastic numerical analyses because three-dimensional finite difference model of the Ilısu dam has a great number of elements and nodes. For this reason, the finite difference mesh is changed several times and a new mesh is created so that the correct result can be achieved and the program will not fail. Total 9 different mesh widths are tried while analyzing. These mesh widths are 50 m, 45 m, 40 m, 35 m, 30 m, 25 m, 20 m, 15 m, 10 m, respectively. It is understood that the settlements on the crest of the Ilısu dam do not change after 10 m mesh width as seen from Fig. 5. So, mesh width is selected 10 m for creep analyses. In addition, time (30 years) is defined to the FLAC3D software using special fish functions and time dependent analyses were performed considering this fish functions.

5. Mathematical formulation

5.1 Interaction condition between discrete surfaces

Interaction condition is very important for large water structures such as CFR dams. This situation occurs between the dam body, foundation and concrete slab for concrete faced rockfill dams. In FLAC3D software, the interaction condition is represented defining normal and shear stiffness values between two discrete planes as seen in Fig. 6.

FLAC3D uses a contact logic which is similar in nature to that used in the different element methods, for either side of the interface. As seen in Fig. 6, gridpoint N is checked for contact on the segment between grid points M and P. If contact is detected, the normal vector (n) is computed for the contact gridpoint (N). In addition, a length (L) is defined for the contact at N along the interface. This length is equal to half of the distance to the nearest gridpoint to the left of N, irrespective of whether the neighboring gridpoint is on the same side of the interface or on the opposite side of N. In this way, the entire interface is divided into contiguous segments, each controlled by a gridpoint. During each time step, the velocity ($\dot{u}$) of each gridpoint is determined as seen at Equal 1. Since the units of velocity are displacement per time step and the calculation of the time step has been scaled to unity to speed convergence. The incremental displacement for any given time step is

$$\Delta u_i \equiv \dot{u}_i \tag{1}$$

The incremental relative displacement vector at the contact point is resolved into the normal and shear directions, and total normal and shear forces are determined by

$$\begin{aligned} F_n^{(t+\Delta t)} &= F_n^{(t)} - k_n \Delta u_n^{(t+(1/2)\Delta t)} L \\ F_s^{(t+\Delta t)} &= F_s^{(t)} - k_s \Delta u_s^{(t+(1/2)\Delta t)} L \end{aligned} \tag{2}$$

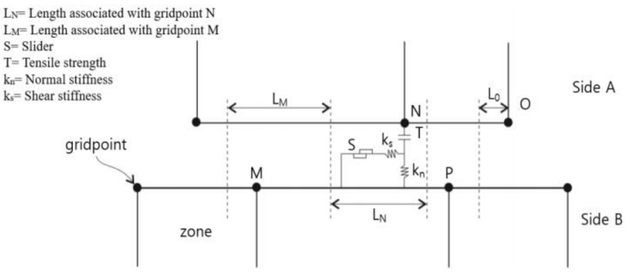

Fig. 6 An interaction condition between A and B sides

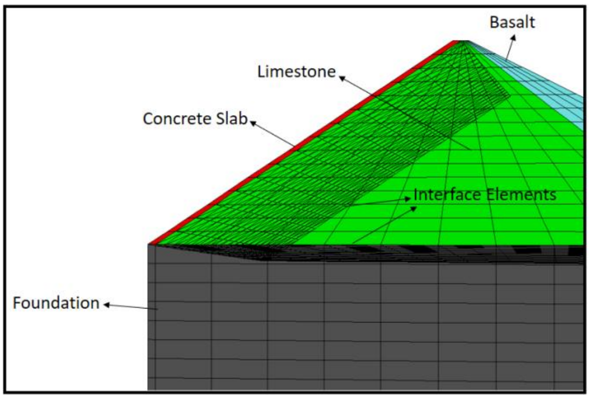

Fig. 7 Interface conditions between dam body-foundation and dam body-concrete slab of the Ilısu dam

Normal (k_n) and shear (k_s) stiffness values are very different for each interface surface. Unit of the k_n and k_s stiffness is stress/displacement (Itasca, 2002). In this study, k_n and k_s stiffness are separately calculated for each discrete surface. These stiffness values are considered as 10^8 Pa/m between the dam body and foundation. Moreover, these values are taken into account as 10^9 Pa/m between the dam body and concrete slab. Shear and normal stiffness values are defined to FLAC3D software using special fish functions.

Normal and shear stiffness (k_n and k_s) are not an easily measured or well-known parameters. Many methods of estimating joint stiffness have been derived in the past. Two important methods are generally used in the numerical analyses. One of them is based on the deformation properties of the rock mass and second one is adopted from the properties of the joint infilling material. These methods are explained in detail as seen below. In addition, interface elements for 3D model of Ilısu CFR dam are shown in Fig. 7.

5.1.1 Calculation of normal and shear stiffness considering rockfill properties

$$\frac{1}{E_m} = \frac{1}{E_i} + \frac{1}{k_n L} \tag{3}$$

where E_m is rock mass modulus; E_i is intact rock modulus; k_n is joint normal stiffness; and L is mean joint spacing. Eq. (3) can be rearranged to obtain the joint normal stiffness as given in Eq. (4).

$$k_n = \frac{E_i E_m}{L(E_i - E_m)} \tag{4}$$

The same expression can be used to derive a relation for the joint shear stiffness as see at Eq. (5).

$$k_s = \frac{G_i G_m}{L(G_i - G_m)} \tag{5}$$

where G_m is rock mass shear modulus; G_i is intact rock shear modulus; and k_s is joint shear stiffness. The equivalent continuum assumption, when extended to three orthogonal joint sets, provides the following relations.

$$\begin{aligned} E_a &= \left(\frac{1}{E_i} + \frac{1}{L_a k_{na}}\right)^{-1} (a = 1,2,3) \\ G_{ab} &= \left(\frac{1}{G_i} + \frac{1}{L_a k_{sa}} + \frac{1}{L_b k_{sb}}\right)^{-1} (a, b = 1,2,3) \end{aligned} \tag{6}$$

Several expressions have been derived for two- and three-dimensional characterizations and multiple joint sets.

5.1.2 Calculation of normal and shear stiffness considering infill properties

Another approach for estimating joint stiffness assumes that a joint has an infill material with known elastic properties. The stiffness of a joint can be evaluated from the thickness and modulus of the infilling material by the following equation.

$$\begin{aligned} k_n &= \frac{E_0}{h} \\ k_s &= \frac{G_0}{h} \end{aligned} \tag{7}$$

where k_n is joint normal stiffness; k_s is joint shear stiffness; E_0 is Young's modulus of infill material; G_0 is shear modulus of infill material; and h is joint thickness or opening.

5.2 The Burger-creep viscoplastic material model

Burger-creep viscoplastic model that is special model for time dependent creep analysis, is characterized with an elasto-plastic volumetric behavior and a visco-elasto-plastic deviatoric behavior. The viscoplastic strain-rate and viscoelastic components are presumed to act in series. The visco-elastic constitutive law corresponds to Burger model (Kelvin and Maxwell components) and the plastic constitutive law corresponds to a Mohr-Coulomb model and burger model. The symbols S_{ij} and e_{ij} are used to denote deviatoric stress and strain components (Itasca 2002).

$$S_{ij} = \sigma_{ij} - \sigma_0 \delta_{ij} \tag{8}$$

$$e_{ij} = \epsilon_{ij} - \frac{e_{vol}}{3} \delta_{ij} \tag{9}$$

where

$$\sigma_0 = \frac{\sigma_{kk}}{3} \tag{10}$$

and

$$e_{vol} = \in_{kk} \tag{11}$$

Kelvin, Maxwell and plastic contributions to stresses and strains are labeled using the superscripts ^{K}, ^{M} and ^{p}, respectively. With those conventions, the model deviatoric behavior may be described by the relations:

Strain rate partitioning

$$\dot{e}_{ij} = \dot{e}_{ij}^{K} + \dot{e}_{ij}^{M} + \dot{e}_{ij}^{p} \tag{12}$$

Kelvin model is expressed as follows

$$S_{ij} = 2\eta^K \dot{e}_{ij}^{K} + 2G^K e_{ij}^K \tag{13}$$

Mohr-Coulomb model is expressed as follows

$$\begin{aligned} \dot{e}_{ij}^{p} &= \lambda^* \frac{\partial g}{\partial \sigma_{ij}} - \frac{1}{3}\dot{e}_{vol}^{p}\delta_{ij} \\ \dot{e}_{vol}^{p} &= \lambda^* \left[\frac{\partial g}{\partial \sigma_{11}} + \frac{\partial g}{\partial \sigma_{22}} + \frac{\partial g}{\partial \sigma_{33}} \right] \end{aligned} \tag{14}$$

Maxwell model is expressed as follows

$$\dot{e}_{ij}^{M} = \frac{\dot{S}_{ij}}{2G^M} + \frac{S_{ij}}{2\eta^M} \tag{15}$$

In turn, the volumetric behavior is given by

$$\dot{\sigma}_0 = K\left(\dot{e}_{vol} - \dot{e}_{vol}^{p}\right) \tag{16}$$

In those formulas, the properties K and G are the bulk and shear moduli, and η is the dynamic viscosity (kinematic viscosity times mass density). The Mohr-Coulomb yield envelope is a composite of shear and tensile criteria. The yield criterion is f=0, and in the principal axes formulation:

Shear yielding

$$f = \sigma_1 - \sigma_3 N_\phi + 2C\sqrt{N_\phi} \tag{17}$$

Tension yielding

$$f = \sigma^t - \sigma_3 \tag{18}$$

where C is the material cohesion, ϕ is the friction, $N_\phi = (1+\sin\phi)/(1-\sin\phi)$, σ^t is the tensile strength, and σ_1, σ_3 are the minimum and maximum principal stresses (compression negative). The potential function g has the form.

Shear failure

$$g = \sigma_1 - \sigma_3 N_\psi \tag{19}$$

Tension failure

$$g = -\sigma_3 \tag{20}$$

where ψ is the material dilation, and $N_\phi = (1+\sin\psi)/(1-\sin\psi)$. Finally, λ^* is a parameter that is nonzero during plastic flow only, which is determined by application of the plastic yield condition f=0 (Itasca 2002).

5.3 Wipp-creep viscoplastic material model

Visco-plasticity can model by combining the viscoelastic WIPP model with the Drucker-Prager plasticity model. The Drucker Prager model is the most compatible with the WIPP-reference creep law, because both models are formulated in terms of the second invariant of the deviatoric stress tensor. The shear yield function for the Drucker-Prager model is

$$f^s = \tau + q_\phi \sigma_0 - k_\phi \tag{21}$$

where f^s= 0 at yield, σ_0= σ_{kk}/3 and $\tau\sqrt{J_2}$ τ where J_2 is the second invariant of the deviatoric stress tensor. Parameters q_ϕ and k_ϕ are material properties.

$$J_2 = \sigma_{ij}^d \sigma_{ij}^d / 2 \tag{22}$$

τ may be related to the stress magnitude, $\bar{\sigma}$

$$\bar{\sigma} = \sqrt{3}\tau \tag{23}$$

The plastic potential function in shear, g^s, is similar to the yield function, with the substitution of q_ψ for q_ϕ as a material property that controls dilation

$$g^s = \tau + q_\psi \sigma_0 \tag{24}$$

If the yield condition (f^s=0) is met, the following flow rules apply

$$\begin{aligned} \dot{\in}_{ij}^{dp} &= \lambda \frac{\partial g^s}{\partial \sigma_{ij}^d} \\ \dot{\in}_{o}^{p} &= \lambda \frac{\partial g^s}{\partial \sigma_o} \end{aligned} \tag{25}$$

where λ is a multiplier (not a material property) to be determined from the requirement that the final stress tensor must satisfy the yield condition. Superscript p denotes "plastic," and d denotes "deviatoric."

$$\begin{aligned} \dot{\in}_{ij}^{dp} &= \lambda \frac{\sigma_{ij}^d}{2\tau} \\ \dot{\in}_{o}^{p} &= \lambda q_\psi \end{aligned} \tag{26}$$

In elastic/plastic formulation, these equations are solved simultaneously with the condition f^s=0, and the condition that the sum of elastic and plastic strain-rates must equal the applied strain-rate. Drucker-Prager model also contains a tensile yield surface, with a composite decision function used near the intersection of the shear and tensile yield functions. The tensile yield surface is

$$f^t = \sigma_o - \sigma^t \tag{27}$$

where σ^t is the tensile yield strength. The associated plastic potential function is

$$g^{t} = \sigma_{o} \tag{28}$$

Using an approach similar to that used for shear yield, the strain rates for tensile yield are

$$\begin{aligned} \dot{\in}_{ij}^{dp} &= 0 \\ \dot{\in}_{o}^{p} &= \lambda \end{aligned} \tag{29}$$

where λ is determined from the condition that f^t=0. Note that the tensile strength cannot be greater than the value of mean stress at which f^s becomes zero.

When both creep and plastic flow occur, it is assumed that the associated strain rates act "in series",

$$\dot{\in}_{ij}^{d} = \dot{\in}_{ij}^{de} + \dot{\in}_{ij}^{dv} + \dot{\in}_{ij}^{dp} \tag{30}$$

where the terms represent elastic, viscous and plastic strain-rates, respectively. We first treat the case of shear yield, f^s > 0,

$$\dot{\in}_{ij}^{d} = \frac{\dot{\sigma}_{ij}^{d}}{2G} + \frac{\sigma_{ij}^{d}}{2\bar{\sigma}}\left(3\dot{\in} + \sqrt{3}\lambda\right) \tag{31}$$

In contrast to the creep-only model, the volumetric response of the viscoplastic model is not uncoupled from the deviatoric behavior unless $q_\psi = 0$ (Itasca 2002).

$$\dot{\in}_{ij}^{d} = \dot{\in}_{ij}^{de} + \dot{\in}_{ij}^{dv} + \dot{\in}_{ij}^{dp} \tag{32}$$

6. Numerical results

Three dimensional (3D) viscoplastic analysis results of the Ilısu CFR dam are presented in this section. Time dependent analyses are performed from 2017 to 2047 due to Ilısu dam was completed in 2017 year. 3D model of the dam is modelled according to original dam project. In the creep analyses, special viscoplastic material models that were rarely used for time dependent analyses of CFR dams are used in the creep analyses and the effects of these material models on the creep behaviour of Ilısu CFR dam are evaluated in detail. Numerical analysis algorithm for viscoplastic analyses is shown in Fig. 8. As the first step of these analyses, only the foundation is collapsed under its self-weight. Then, all displacements which are obtained from the collapsed model are set to zero. This process is implemented in order to exclude construction related deformations. Afterwards, the dam body is placed on the settled foundation model and foundation-dam body system is collapsed under its self-weight. As a consequence, behaviour of the dam is evaluated for empty reservoir condition of the dam. According to second step of the numerical analyses, the reservoir water is modelled and foundation-dam body-reservoir interaction system of Ilısu dam is analyzed during 30 years for 120 m (maximum reservoir height) of the reservoir water height. According to time dependent analyses, settlements, horizontal displacements, principal stresses and pore pressures which

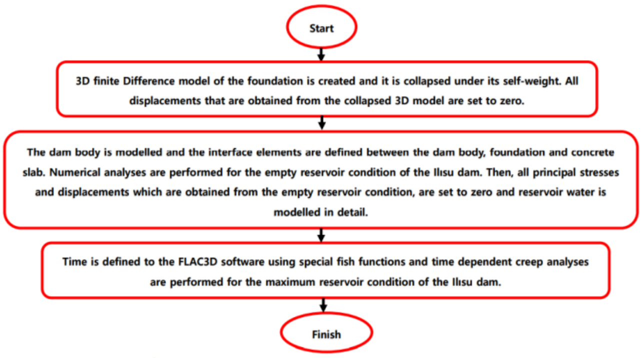

Fig. 8 Numerical analysis algorithm for viscoplastic creep analyses

may take place from 2017 to 2047 are evaluated for maximum reservoir condition of the dam in detail. In addition, results are compared for empty and maximum reservoir condition of the dam as follows subsections.

6.1 Empty reservoir condition of the dam

Deformation monitoring is one of the most important method for analyzing the deformation characteristics of dams and it provides a warning system for abnormal behaviour of the dam (Cetin *et al.* 2000, Szostak and Massiera, 2006). So, observing time dependent behaviour and the deformation of the dam body are vital for safety of these structures. In this section, vertical-horizontal displacements and maximum principal stresses are shown for initial condition (empty reservoir condition) of the dam in Figs. 9-12. According to Fig. 9, maximum vertical displacement took place at the crest point of the dam and approximately 60 cm settlement is observed on this point. In addition, 42 cm and 28 cm vertical displacements occurred at the middle and bottom of the dam body, respectively. About 10 cm settlement is observed on the surface of the foundation and settlements diminished from the surface to bottom of the foundation. The dam body is divided into two parts from the midpoint of the center to examine the behavior changes in the dam body in detail and it is clearly seen that the vertical displacements decreased from the crest to the foundation. Because of the dam body and foundation is not exposed to any external force (e.g., hydrostatic pressure), too small vertical displacements occurred on the surface of the foundation (Fig. 9). Furthermore, when the vertical displacement vectors are examined, it is observed that direction of the displacement vectors is the vertical direction in the dam body and foundation. The largest vector is obtained at the crest point of the dam as seen from Fig. 10 and the size of vectors decreased from the crest to foundation.

Horizontal displacements and principal stresses for empty reservoir condition are shown in Figs. 11 and 12, respectively. When the numerical results are examined, in spite of horizontal displacements occurred in the negative direction in the upstream side of the dam, displacements took place in the opposite direction (positive) at the downstream side. It is clearly appeared that the horizontal displacements increased from the crest to the foundation

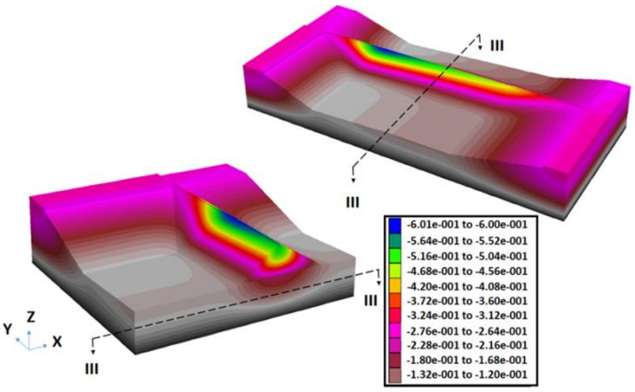

Fig. 9 Vertical displacements (m) for empty reservoir condition of the dam

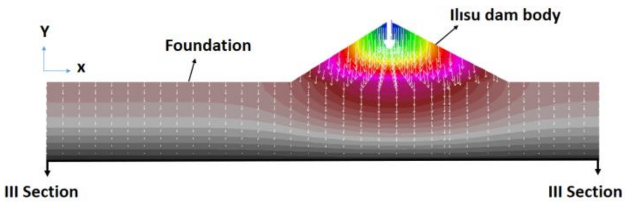

Fig. 10 Vertical displacement vectors for III-III section of the dam

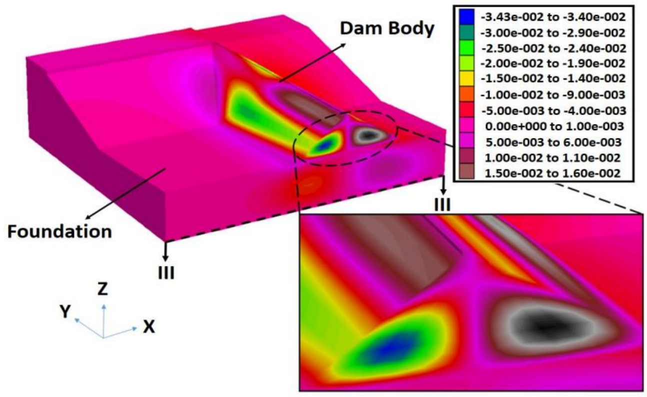

Fig. 11 Horizontal displacements (m) for empty reservoir condition of the dam

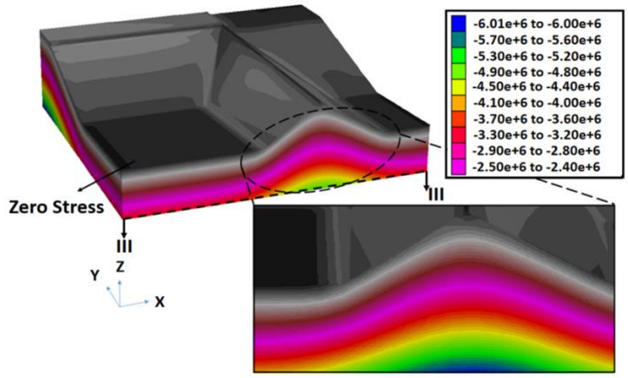

Fig. 12 Maximum principal stresses (Pa) for empty reservoir condition of the dam

and minimum displacement values are observed at the crest of the dam as seen from Fig. 11. 3.47 cm horizontal displacement is obtained from numerical analyses at the upstream side of the dam for the empty reservoir condition of the dam. Moreover, it is obviously seen that more horizontal displacements are observed at upstream side of the dam compared with downstream side (Fig. 11). 1.5 cm horizontal displacement occurred at the downstream side of the dam and any displacement did not take place on the foundation. According to the principal stress results, any stresses did not occur on the surface of the dam body and the principal stresses increased from the crest to the foundation as seen from Fig. 12. When investigated the split half condition of the dam, about 6.01 Mpa maximum stress is observed at the bottom of the foundation and 2.5 Mpa principal stress took place at bottom of the dam body for empty reservoir condition. In addition, any principal stress did not take place on the surface of the foundation due to external loads did not expose to these surface. Principal stresses increased from the surface to the bottom of the foundation (Fig. 12).

6.2 Maximum reservoir condition of the dam

Hydrostatic pressure is an important factor in settlement of the CFR dams (Zhou *et al.* 2011). Thus, the effect of hydrostatic pressure and water flowing on the dam behaviour is examined in detail in this section. Firstly, all displacements (vertical and horizontal) and principal stresses which are obtained from the empty reservoir condition of the dam are set to zero in order to exclude construction related the stresses and deformations. Then, reservoir water is modelled considering maximum reservoir level and effect of the pore pressure is taken into account in the all viscoplastic analyses. While modelling reservoir water, water table and hydrostatic water loads are defined to the 3D model using special fish functions. Vertical displacement results of the dam are shown in Fig. 13-16. According to time dependent numerical results, it is clearly seen that more settlements occurred in the dam body for maximum reservoir condition when compared with empty reservoir condition. Maximum settlements occurred on the crest point of the dam and approximately 67 cm maximum vertical displacement is observed at this point. In spite of any settlement did not take place on the surface of foundation for empty reservoir situation of the dam, approximately 30 cm settlement is observed on the surface of the foundation (on upstream surface of the dam) for maximum reservoir condition (Fig. 13). When compared upstream and downstream side of the dam, it is obviously seen that more settlements occurred at the upstream side of the dam due to effect of the hydrostatic pressure as seen in Fig 13. In addition, 38 cm and 56 cm vertical displacements are observed at bottom of the dam body and middle of the dam body, respectively.

Reservoir water loads altered the direction of settlement vectors at the foundation and dam body for maximum reservoir condition if compared with the empty reservoir condition. In spite of vertical settlement vectors occurred in the dam body for empty condition, traverse displacement vectors observed in the dam for maximum reservoir water condition by effect of the hydrostatic pressure, water flow and leakage (Fig. 14). Besides, deformed situation of the dam during 30 years is shown in Fig. 15. Bottom of the dam body is more deformed than the crest and deformation size

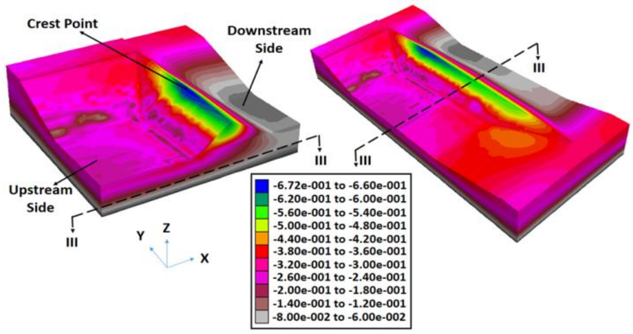

Fig. 13 Vertical displacement results for the maximum reservoir condition of the dam

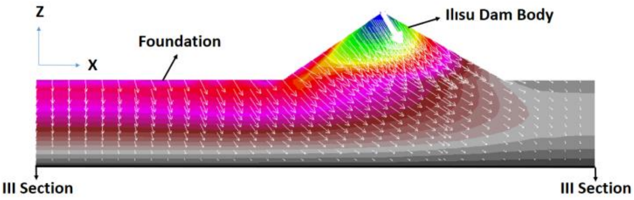

Fig. 14 Vertical displacement vectors of III-III section for maximum reservoir condition of the dam

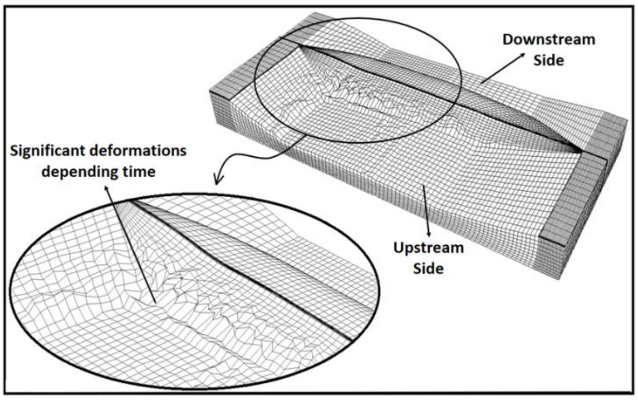

Fig. 15 Deformed condition of the dam for maximum reservoir condition

is very critic at bottom of the dam. In addition, remarkable deformations are observed on the surface of the foundation as seen Fig. 15.

All fluid analyses are performed depending the time in order to see deterioration of the rockfill materials in time. Numerical analyses were started from 2017 year because of Ilısu dam was completed in 2017 year and analyses were finished at 2047 year. One of the most important aims of this study is to observe the viscoplastic behaviour changes of the dam during 30 years. Time is defined to FLAC3D using fish codes which can specifically defined to software and time dependent deformations are observed for 4 points under the concrete slab of the dam body graphically. Details are shown in Fig. 16. When examined the time dependent settlements of the 4 points on the most critical section of the dam during 30 years, it is clearly seen that settlements change continued during 21 years. In the other word, settlements will increase from 2017 to 2038 and settlement changes will diminish after 2038. This results are very important to evaluate the future of Ilısu CFR dam.

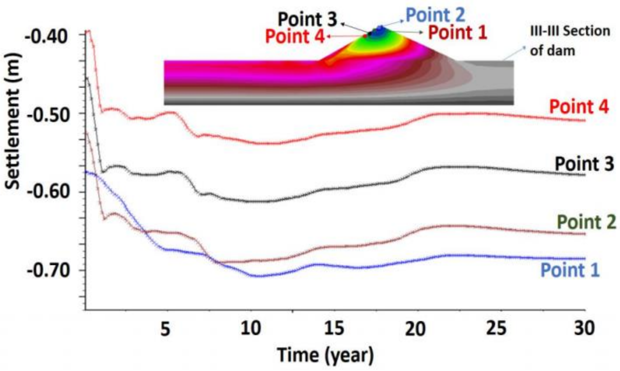

Fig. 16 Time dependent vertical displacements (m) for 4 nodal points under the concrete slab

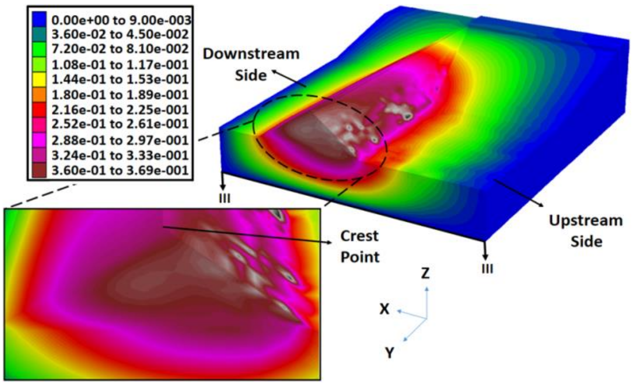

Fig. 17 Horizontal displacements (m) for maximum reservoir condition of the dam

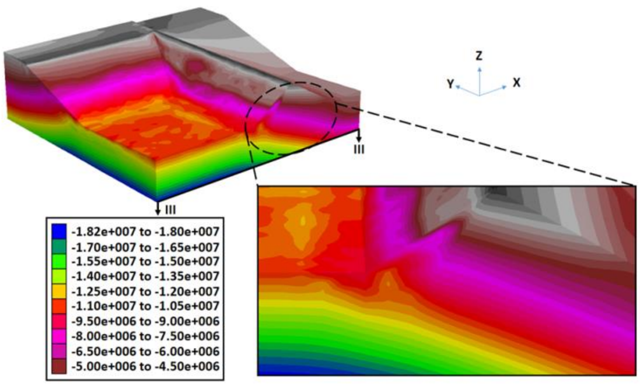

Fig. 18 Maximum principal stresses (Pa) for maximum reservoir condition of the dam

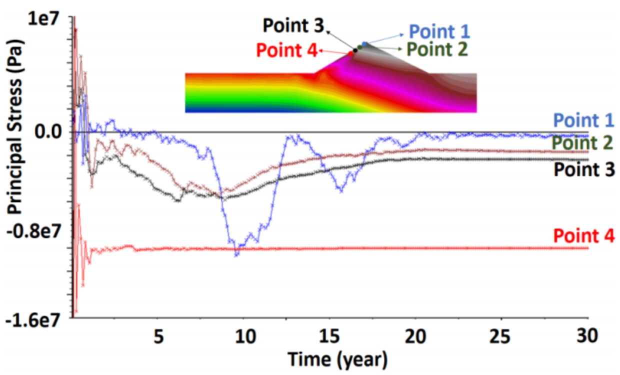

Fig. 19 Time dependent principal stresses (Pa) for 4 points under the concrete slab

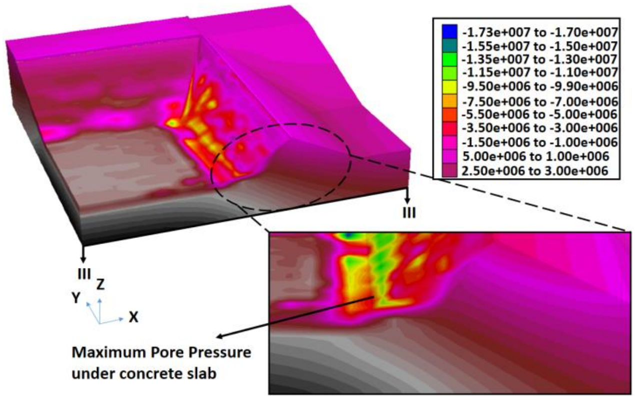

Fig. 20 Pore pressure (Pa) for maximum reservoir condition of the dam

Maximum and minimum vertical displacements are observed on the Point 1 (crest of the dam) and Point 4 (bottom of the dam), respectively. Moreover, 52 cm and 68 cm maximum settlements occurred at the Point 4 and Point 1, respectively as seen from Fig. 16.

Time depending horizontal displacement results are presented in Fig. 17. It is clearly seen from Fig. 17 that when compared with empty condition of the dam, more horizontal displacements are observed in the dam body for maximum reservoir condition. 36.9 cm maximum displacement occurred under the crest of the dam. In despite of any displacements did not take place on the surface of the foundation for empty reservoir condition, approximately 14 cm horizontal displacement is occurred for the maximum reservoir condition. Besides, 26 cm displacement is observed at middle of the dam body and all displacements took place in positive direction (*x* direction) according to time depending viscoplastic analyses as seen Fig. 17. This result proved the effect of hydrostatic pressure on the horizontal displacement behaviour of Ilısu CFR dam.

In Fig. 18, the effect of hydrostatic water loads on the creep behaviour of Ilısu CFR dam is clearly seen. It is obviously understood from Fig. 18 that when compared with empty reservoir condition, principal stresses in the dam body increased and directions of the contour lines obviously changed for the maximum reservoir condition. 18.27 Mpa principal stress is observed at the bottom of the foundation for maximum reservoir condition and more stresses occurred on the surface of foundation compared with the empty reservoir condition. 11 Mpa principal stress is observed on the surface of the foundation. In addition, 5 Mpa and 8 Mpa principal stresses are obtained from numerical analyses for the crest and middle of the dam, respectively. Minimum stresses are occurred at the downstream side of the dam (Fig. 18). Principal stresses of 4 points during 30 years is graphically shown in Fig. 19. When examined this graphic, maximum and minimum stresses are observed at the Point 4 and Point 1, respectively. It is obviously seen from this result that hydrostatic pressure increases from crest to bottom of the dam depending to the reservoir height. Principal stress changes continued during 21 years (from 2017 to 2038) according to fluid analyses (Fig. 19) and changes diminished after this time (between 2038 and 2047). Significant principal stress changes occurred at the crest point as seen in Fig. 19. Pore pressure is examined for under the concrete slab of the dam. According to the fluid analyses, pore pressure contour lines took place from the upstream side to the downstream side and 10 Mpa pore pressure is observed bottom of the foundation. Moreover, for dam body surface, maximum pore pressure is obtained on the middle of the dam body surface and minimum pressure is obtained at the crest of the dam as seen Fig. 20. This result is shown that effects of the water flow and leakage alter the behaviour of the dam and it is vital important for modelling of the concrete faced rockfill dams.

7. Conclusions

Deformation control and monitoring are vital important for the high and long concrete faced rockfill dams (e.g., Ilısu CFR dam). For this purpose, the principal stresses, horizontal displacements, vertical displacements and pore pressures of the Ilısu dam are analyzed by 3D numerical modelling and viscoplastic behaviour of the Ilısu dam is examined and evaluated depending the time in detail in this study. Specific material models that rarely used for the creep analyses of CFR dams are considered for time dependent analyses and material properties are selected from experimental data. Firstly, numerical analyses are performed for empty reservoir condition of the dam. Then, reservoir water is modelled taking into account water table and hydrostatic water loads and viscoplastic creep analyses are performed for maximum reservoir condition (120 m) depending to the time in order to see deterioration of the rockfill materials in time. Numerical analyses are started from 2017 year because of Ilısu dam was completed in 2017 year and analyses continued until 2047 year. Principal stresses, settlements, horizontal displacements and pore pressure which occurred due to effect of the hydrostatic pressure and leakage are evaluated according to numerical analyses in detail. These important results are assessed as below:

- Two different special viscoplastic material models were used in this study. These material models are Burger and WIPP creep material models. It is clearly observed that Burger viscoplastic model should be used for rockfill materials of CFR dams in the creep analyses. Moreover, Wipp- creep viscoplastic model should be considered for concrete slab in time dependent analyses of CFR dams.
- According to numerical analysis results, large settlement differences are observed between the empty and maximum reservoir condition of the dam. Time dependent behaviour of the dam clearly changed after the dam started to hold the water and more settlements occurred in the dam body for maximum reservoir condition when compared with empty reservoir condition. Maximum settlement took place on the crest point of the dam for empty and maximum reservoir conditions. In addition, in spite of vertical settlement vectors occurred in the dam body for empty condition, traverse displacement vectors observed in the dam body for maximum reservoir water condition by effect of the hydrostatic pressure and water flow.
- 4 points on the dam body surface are selected from

under the concrete slab in order to better observe the time dependent viscoplastic behaviour changes of the dam. When examined time dependent settlements of these points during 30 years for maximum reservoir condition, 68 cm maximum vertical displacement is observed at Point 1 (top nodal point) and 52 cm settlement occurred at Point 4 (lowest nodal point). In addition, vertical displacements increased until a certain time and the changes decreased after this time. In the other word, settlements will increase from 2017 to 2038 and settlement changes will diminish after 2038. This results are very important to evaluate the future of Ilısu CFR dam.

• According to horizontal displacement results, when compared with empty reservoir condition, more displacements are observed on the dam body surface by effect of the hydrostatic pressure for maximum reservoir condition. For empty reservoir condition, although horizontal displacements took place in the negative direction in the upstream side of the dam, displacements occurred in the positive direction at the downstream side. However, for maximum reservoir condition, direction of the displacements for both side of the dam body is in positive direction (from upstream to downstream). This result shows the effect of hydrostatic pressure on the horizontal displacement behaviour of Ilısu CFR dam.

• Significant deformations are observed at bottom of the dam body surface depending to the time. Moreover, remarkable deformations occured on the surface of foundation. This result is clearly indicated the effect of water loads on the deformation behaviour of Ilısu CFR dam.

• For empty reservoir situation, any principal stresses are not observed on the surface of the dam body because of external loads (eg. hydrostatic pressure) did not expose to these surface and stresses increased from crest to bottom of the dam body surface. After reservoir water exposed to surface of the dam, principal stresses increased and time dependent stress behaviour of the dam clearly changed.

• In order to better seen pore pressure changes of the dam, 4 nodal points are selected under the concrete slab. According to the fluid analyses, minimum pore pressure is observed at the crest of the dam and maximum pore pressure occurred at middle of the dam body surface. This result is shown the effect of the water flowing on the time dependent pore pressure behaviour of Ilısu CFR dam.

References

Albaa, M., Bernardinib, G., Giussania, A., Riccip, P.P, Roncoronia, F., Scaionia, M., Valgoic, P. and Zhang, K. (2008), "Measurement of dam deformations by terrestrial interferometric techniques" *Proceedings of the 21st ISPRS Congress*, Beijing, China, July.

Baak, S.H., Cho, G.C. and Song, K.I. (2009), "Stability analysis on the concrete slab of the highest concrete-faced rock-fill dam in South Korea", *Geomech. Eng.*, **13**(5), 881-892.

Bayraktar, A., Kartal, M.E. and Basaga, H.B. (2009), "Reservoir water effects on earthquake performance evaluation of Torul concrete-faced Rockfill dam", *Water Sci. Eng.*, **2**(1), 43-57.

Cetin, H., Laman, M. and Ertunç, A. (2000), "Settlement and slaking problems in the world's fourth largest rock-fill dam, the Ataturk Dam in Turkey", *Eng. Geol.*, **56**(3-4), 225-242.

Clements, R.P. (1984), "Post-construction deformation of rockfill dams", *J. Geotech. Eng.*, **110**(7), 821-840.

Dakoulas, P. (2012), "Nonlinear seismic response of tall concrete-faced rockfill dams in narrow canyons", *Soil Dyn. Earthq. Eng.*, **34**(1), 11-24.

DSI (2018), *General Directorate of State Hydraulic Works*, Regional Directorate, Ankara, Turkey.

Duncan, J.M. (1996), "State of the art: limit equilibrium and finite element analysis of slopes", *J. Geotech. Eng.*, **122**(7), 577-595.

Fang, C. and Liu, Z. (2011), "Stress-strain analysis of Aikou rockfill dam with asphalt-concrete core", *J. Rock Mech. Geotech. Eng.*, **3**(2), 186-192.

Fenves, G.L. (1998), "Plastic-damage model for cyclic loading of concrete structures", *J. Eng. Mech.*, **124**(8), 892-900.

Guo, Q., Pei, L., Zhou, Z., Chen, J. and Yao, F. (2016), "Response surface and genetic method of deformation back analysis for high core rockfill dams", *Comput. Geotech.*, **74**, 132-140.

Itasca Consulting Group Inc. (2002), *FLAC version 5 User Manual*, Itasca Consulting Group, Inc., Minneapolis, U.S.A.

Kartal, M.E., Cavusli, M. and Sunbul, A.B. (2017), "Assessing seismic response of a 2D roller-compacted concrete dam under variable reservoir lengths", *Arab. J. Geosci.*, **10**(22), 488.

Kim, Y.S., Seo, M.W., Lee, C.W. and Kang, G.C. (2014), "Deformation characteristics during construction and after impoundment of the CFRD-type Daegok Dam, Korea", *Eng. Geol.*, **178**, 1-14.

Kovacevic, N., Potts, D.M. abd Vaughan, P.R. (1994), "Finite element analysis of a rockfill dam", *Proceedings of the 8th International Conference on Computer Methods and Advances in Geomechanics*, Morgantown, U.S.A.

Li, G.C. and Desai, C.S. (1983), "Stress and seepage analysis of earthen dams", *J. Geotech. Eng.*, **109**(7), 946-960

Mahinroosta, R., Alizadeh, A. and Gatmiri, B. (2015), "Simulation of collapse settlement of first filling in a high rockfill dam", *Eng. Geol.*, **187**, 32-44.

Naylor, D.J. (1997), *Collapse Settlement-Some Developments*, in *Applications on Computational Mechanics in Geotechnical Engineering*, A.A. Balkema, Rotterdam, The Netherlands, 37-54.

Pang, R., Xu, B., Zou, D. and Kong, X. (2018), "Stochastic seismic performance assessment of high CFRDs based on generalized probability density evolution method", *Comput. Geotech.*, **97**, 233-245.

Pang, R., Xu, B., Kong, X. and Zou, D. (2018), "Seismic fragility for high CFRDs based on deformation and damage index through incremental dynamic analysis", *Soil Dyn. Earthq. Eng.*, **104**, 432-436.

Pang, R., Xu, B., Kong, X., Zou, D. and Zhou, Y. (2018), "Seismic reliability assessment of earth-rockfill dam slopes considering strain-softening of rockfill based on generalized probability density evolution method", *Soil Dyn. Earthq. Eng.*, **107**, 96-107.

Pramthawee, P., Jongpradist, P. and Sukkarak, R. (2017), "Integration of creep into a modified hardening soil model for time-dependent analysis of a high rockfill dam", *Comput. Geotech.*, **91**, 104-116.

Rashidi, M. and Haeri, S.M. (2017), "Evaluation of behaviors of earth and rockfill dams during construction and initial impounding using instrumentation data and numerical modeling", *J. Rock Mech. Geotech. Eng.*, **9**(4), 709-725.

Seo, M.W., Ha, I.S., Kim, Y.S. and Olson, S.M. (2009), "Behavior of concrete-faced rockfill dams during initial impoundment", *J. Geotech. Geoenviron. Eng.*, **135**(8), 1070-1081.

Soydemir, C. and Kjaernsli, B. (1979), "Deformation of membrane-faced rockfill dams", *Proceedings of the 7th European Conference on Soil Mechanics and Foundation Engineering*, Brighton, England, September.

Szostak-Chrzanowski, A. and Massiéra, M. (2006), "Relation between monitoring and design aspects of large earth dams", *Proceedings of the 3rd IAG Symposium on Geodesy for Geotechnical and Structural Engineering and 12th FIG Symposium on Deformation Measurements*, Bauden, Austria, May.

Wen, L., Chai, J., Xu, Z., Qin, Y. and Li, Y. (2017), "Monitoring and numerical analysis of behaviour of Miaojiaba concrete-face rockfill dam built on river gravel foundation in China", *Comput. Geotech.*, **85**, 230-248.

Xu, B., Zou, D. and Liu, H. (2012), "Three dimensional simulation of the construction process of the Zipingpu concrete face rockfill dam based on a generalized plasticity model", *Comput. Geotech.*, **43**, 143-154.

Xu, B., Zou, D., Kong, X. and Zhou, Y. (2017), "Concrete slab dynamic damage analysis of CFRD based on concrete nonuniformity", *Int. J. Geomech.*, **17**(9), 04017055.

Xu, B., Zou, D., Kong, X., Hu, Z. and Zhou, Y. (2015), "Dynamic damage evaluation on the slabs of the concrete faced rockfill dam with the plastic-damage model", *Comput. Geotech.*, **65**, 258-265.

Yu, Y., Xie, L. and Zhang, B. (2005), "Stability of earth-rockfill dams: Influence of geometry on the three dimensional effect", *Comput. Geotech.*, **32**, 326-339.

Zhang, B., Wang, J.G. and Shi, R. (2004), "Time-dependent deformation in high concrete-faced rockfill dam and separation between concrete face slab and cushion layer", *Comput. Geotech.*, **31**, 559-573.

Zhou, W., Hua, J., Chang, X. and Zhou, C. (2011), "Dam-reservoir-foundation interaction effects on the modal characteristic of concrete gravity dams", *Struct. Eng. Mech.*, **38**(1), 65-79.

Zhou, M.Z., Zhang, B.Y. and Jie, Y.X. (2016), "Numerical simulation of soft longitudinal joints in concrete faced rockfill dam", *Soil. Found.*, **56**(3), 379-390.

Zou, L., Wang, S. and Lai, X. (2013), "Creep model for unsaturated soils in sliding zone of Qianjiangping landslide", *J. Rock Mech. Geotech. Eng.*, **5**(2), 162-167.

Zou, D., Xu, B., Kong, X., Liu, H. and Zhou, Y. (2013), "Numerical simulation of the seismic response of the Zipingpu concrete face rockfill dam during the Wenchuan earthquake based on a generalized plasticity model", *Comput. Geotech.*, **49**, 111-122.

CC